AFRL-RB-WP-TP-2009-3016

ON THE DESIGN OF HYPERSONIC INWARD-TURNING INLETS

Capt. Barry A. Croker

Aerospace Vehicle Integration and Demonstration Branch
Aeronautical Sciences Division

JUNE 2007

Approved for public release; distribution unlimited.
See additional restrictions described on inside pages

STINFO COPY

AIR FORCE RESEARCH LABORATORY
AIR VEHICLES DIRECTORATE
WRIGHT-PATTERSON AIR FORCE BASE, OH 45433-7542
AIR FORCE MATERIEL COMMAND
UNITED STATES AIR FORCE

REPORT DOCUMENTATION PAGE	*Form Approved* *OMB No. 0704-0188*

1. REPORT DATE *(DD-MM-YY)*	2. REPORT TYPE	3. DATES COVERED *(From - To)*
June 2007	Conference Paper Preprint	01 September 2006 – 01 May 2007

4. TITLE AND SUBTITLE ON THE DESIGN OF HYPERSONIC INWARD-TURNING INLETS	**5a. CONTRACT NUMBER** In-house **5b. GRANT NUMBER** **5c. PROGRAM ELEMENT NUMBER** N/A
6. AUTHOR(S) Capt. Barry A. Croker	**5d. PROJECT NUMBER** A0AI **5e. TASK NUMBER** **5f. WORK UNIT NUMBER** 0A
7. PERFORMING ORGANIZATION NAME(S) AND ADDRESS(ES) Aerospace Vehicle Integration and Demonstration Branch (AFRL/RBAI) Aeronautical Sciences Division, Air Force Research Laboratory Air Vehicles Directorate Wright-Patterson Air Force Base, OH 45433-7542 Air Force Materiel Command, United States Air Force	**8. PERFORMING ORGANIZATION REPORT NUMBER** AFRL-RB-WP-TP-2009-3016
9. SPONSORING/MONITORING AGENCY NAME(S) AND ADDRESS(ES) Air Force Research Laboratory Air Vehicles Directorate Wright-Patterson Air Force Base, OH 45433-7542 Air Force Materiel Command United States Air Force	**10. SPONSORING/MONITORING AGENCY ACRONYM(S)** AFRL/RBAI **11. SPONSORING/MONITORING AGENCY REPORT NUMBER(S)** AFRL-RB-WP-TP-2009-3016

12. DISTRIBUTION/AVAILABILITY STATEMENT
Approved for public release; distribution unlimited.

13. SUPPLEMENTARY NOTES
PAO Case Number: AFRL/WS 2007-0369, 23 Feb 2007. Report contains color.

Conference paper presented at the 3rd Annual Symposium on Integrating CFD and Experiments in Aerodynamics, which was held at the Air Force Academy in June 2007.

14. ABSTRACT
A family of dual-axis compression, high-contraction-ratio, inward-turning inlets has been designed to achieve a desired shock structure and aerodynamic performance at Mach 6. Computational simulations of the internal inlet flowfield were performed using the research code FDL3DI. These solutions are an integrated part of the inlet design methodology and offer insight into the fundamental fluid phenomenology. The effects of viscous/inviscid interactions, namely swept-shock/turbulent boundary layer interactions are discussed. Additionally, the importance of complementary computational fluid dynamics (CFD) to the experimental work as part of the integrated hypersonic inlet design process is also addressed.

15. SUBJECT TERMS
hypersonics, inlet design inward-turning, SWBLI

16. SECURITY CLASSIFICATION OF:			17. LIMITATION OF ABSTRACT:	18. NUMBER OF PAGES	19a. NAME OF RESPONSIBLE PERSON (Monitor)
a. REPORT	b. ABSTRACT	c. THIS PAGE			Heidi Wilkin
Unclassified	Unclassified	Unclassified	SAR	18	**19b. TELEPHONE NUMBER** *(Include Area Code)* N/A

Standard Form 298 (Rev. 8-98)
Prescribed by ANSI Std. Z39-18

On the Design of Hypersonic Inward-Turning Inlets

Capt. Barry. A. Croker, Deputy Chief

Aerospace Vehicle Integration and Demonstration Branch
Air Vehicles Directorate
Air Force Research Laboratory
Wright-Patterson AFB, OH 45433
barry.croker@wpafb.af.mil

Abstract

There has been a recent re-emphasis in the exploration of hypersonic inlets utilizing circular or elliptical cross sections due to advantages in structural integrity, flow distortion and propulsive efficiencies as compared with similar rectangular devices. A family of dual axis compression, high contraction ratio inward-turning inlets has been designed to achieve a desired shock structure and aerodynamic performance at Mach 6. Computational simulations of the internal inlet flow fields are performed using the research code FDL3DI for design methodology validation and fundamental physical insight. A subscale test article is planned for testing in the NASA Langley 20 Mach 6 wind tunnel, to collect data to quantify inlet performance, assess computational predictive capabilities, and verify design methodologies. The effect of viscous/invisicid interactions, namely swept-shock/turbulent boundary layer interactions are discussed. The importance of complementary CFD and experiments in the integrated hypersonic inlet design process is also addressed.

Key words: Hypersonics, Inlet Design, Inward-Turning, SBLI

Introduction

The future capability vision of the U.S. Air Force includes revolutionary concepts to provide unparalleled global reach and power for our nations armed forces. Three of these include Prompt Global Strike delivering rapid-response kinetic kill capabilities, Operationally Responsive Access to Space for economically viable reusable spacelift, and Long Range Strike capable of providing desired effects anywhere on the globe within hours of tasking. Realization of these ob jectives will yield a full spectrum aerospace power able to rapidly pro ject lethal force across a seamless aerospace continuum. High speed vehicles capable of survivable, air-breathing flight enable these transformational capabilities by facilitating conventional munition strike with adaptive target selection, establishment of adversary exclusion zones and global strike ability with CONUS-based assets. Near term capability requirements dictate the development of expendable missile-scale vehicles for intra-theater standoff operations, while far term ob jectives focus on reusable global cruiser-like platforms utilizing integrated combined cycle flow paths for hypersonic and exo-atmospheric operations. Clearly the premise of sustainable hypersonic air-breathing flight is a key enabling technology for the effectuation of these visions.

Of current interest to the Air Force Research Lab are circular, inward-turning inlet systems designed for vehicles operating between Mach 6 and Mach 12. Inward-turning designs are delineated from their axis-symmetric counterparts by the use of internal geometries which direct compression towards the flow centerline similar to a traditional rectangular inlet, but with a non-rectangular cross-section. Particularly attractive characteristics include the elimination of low momentum corner flows, reduced wetted area for lower drag and cooling requirements, and decreased vehicle weight due to the inherent strength of round versus rectangular cross sections. Preliminary numerical design studies have shown that inward-turning designs can result in lower flow field distortion and greater propulsive efficiencies than similar rectangular devices[1]. The potential of inward-turning geometries was also demonstrated by NASAs Rectangular to Elliptical Shape Transition (REST) inlet program, which proved that a fixed-geometry inward-turning inlet could provide performance and operability over a variable flight envelope[2, 3, 4].

Inlet Design

At this time significant technical challenges remain associated with the practice of hypersonic air-breathing flight. A myriad of complexities and complications with respect to thermal management, hypersonic aerodynamics, aerothermodynamics, and aero-propulsion integration have inhibited routine operations within the hypersonic regime. A combination of these last three challenges exists in the determination and integration of optimized inlet configurations on realistic flight vehicles. Because of the complex interactions and dependencies found in hypersonic flows, the typical delineation between airframe and propulsion which is possible in low-speed flight is no longer possible in a high-speed vehicle. The complete flowpath must therefore be designed in an integrated fashion.

Traditional integration tools often oversimplify the non-linear and non-equlibrium phenomena encountered in hypersonic flows and thus can produce inoperable or inefficient designs when applied to high speed regimes. To overcome these deficiencies, high-fidelity three-dimensional simulations can be utilized to model fundamental physical behavior. Recent numerical studies have demonstrated the negative impact of non-ideal fluid dynamics on the aerodynamic and propulsive performance of traditionally-optimized designs [1]. Separate research has clarified the effects of distortion in degrading thermal and energy management techniques of advanced plasma-based control methods [5]. Notwithstanding, computational studies are not the panacea of aero-propulsion integration and need to be judiciously complemented by experimental studies to ensure the validity of chosen numerical models. It is the intent of this paper to document a complementary computational/experimental hypersonic inlet design process, highlighting the capabilities and deficiencies of each method.

JAWS

The moniker "JAWS" refers to a family of inward-turning, dual-axis compression fixed geometry inlets developed by AFRL based on the historical work of Kutschenreuter et al.[6]. Since the flow path geometry is fixed, specific inlet designs are optimized for operation at finite flight conditions chosen *a priori*. However, the overall design methodology can be applied to any chosen flight condition and thus produce a family of inlet geometries.

The design process begins with a target freestream Mach number and dynamic pressure, along with a desired combustor Mach number and geometry. For the current research, the freestream conditions were chosen to match available experimental facilities, with $M = 6.0$ and $Q = 1000$ psf. A circular exit profile was chosen to match a complimentary circular combustor interface. An inviscid compressive flow-field is then chosen starting with the freestream conditions which using a series of oblique shocks terminates at the desired combustor Mach number. Invisicid streamlines at the perimeter of the combustor interface are then traced backwards through the compressive flow-field to define the outer radius of the inlet cross-sectional areas. Finally, the leading edge of the inlet is defined by the initial intersection of the calculated stream traces and the primary oblique shock. In a traditional two-dimensional rectangular inlet, compression is induced primarily by the upper and/or lower inlet surfaces. These surfaces are nominally planar and in turn create planar shocks. In the JAWS inlet, this method of stream tracing results in a three-dimensionally curved compression surface but a planar shock structure. As the shock angles and strengths in the compressive flow-field are adjusted, the resulting shape of the inlet leading edge profile can be tailored as needed. For the JAWS inlet, the majority of the compression comes through two separate oblique shock trains in the y and z planes, carefully tuned such the initial inlet cross section is also circular.

Figure 1a shows several views of the finalized JAWS geometry. Most notable about the design are the upper and lower capture surfaces which form the characteristic "jaws" of the inlet. The convergence of the upper and lower surfaces to a sharp corner at the x-z symmetry plane is referred to as the "crotch" of the inlet. After the crotch there is relief in the vertical contraction, but additional compression in the horizontal direction. The shift between vertical and horizontal compression can be see in the red cross-sectional planes in Figure 1b. Note that while there are significant three-dimensional changes to the internal profile of the inlet, both the initial capture area and the downstream exit remain circular in profile.

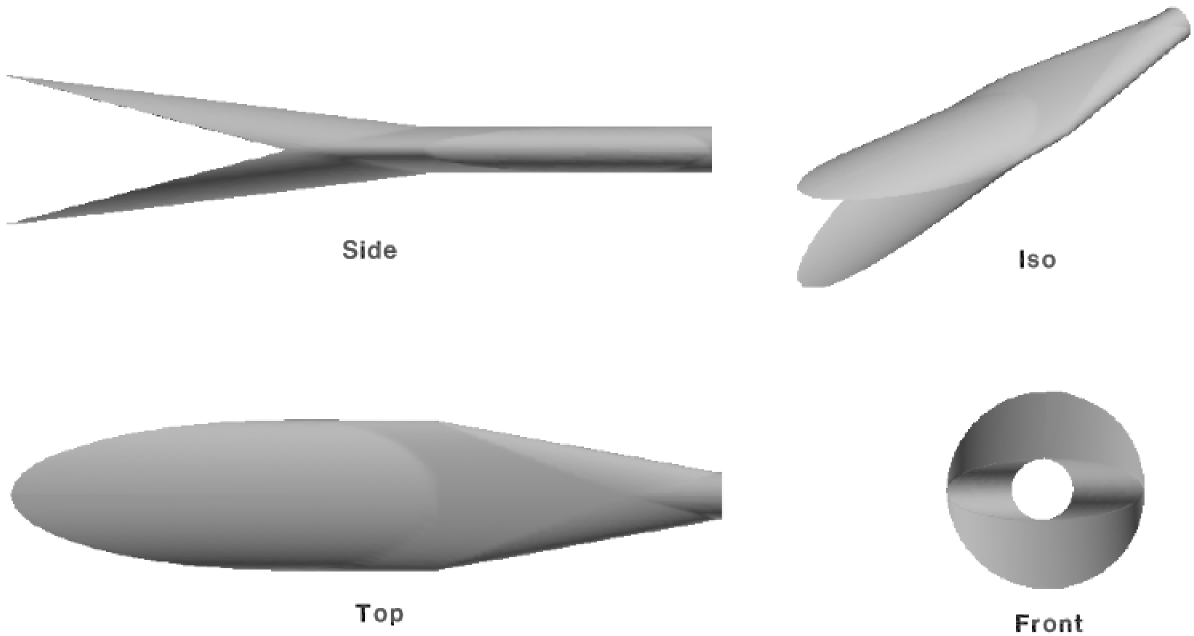

(a) Exterior Surfaces

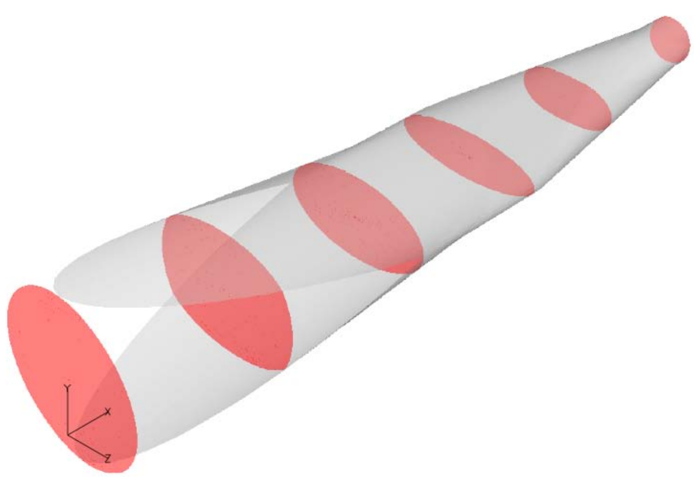

(b) Internal Profiles

Figure 1: **JAWS Inlet Geometry**

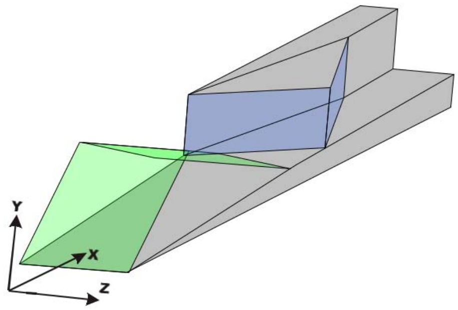

(a) Quarter-section Analogy

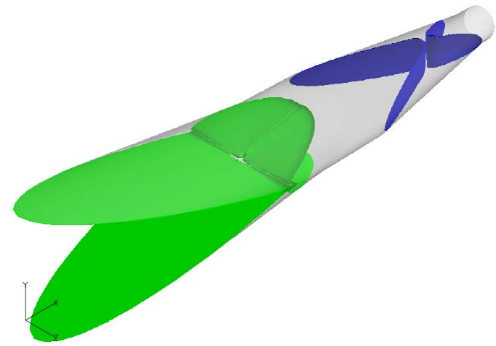

(b) 3D JAWS

Figure 2: **JAWS Shock Topology**

In order to clearly visualize the shock structure formed by the interior compression surfaces, a quarter section of an analogous rectangular representation is shown in Figure 2a. The flow is first turned in the y-direction direction forming a x-z planar shock, as denoted by the green surface. There is a corresponding compression surface at the top of the inlet, and the pair of planar shock meet and then reflect at the x-z centerline plane. This shock train will be referred to as the primary shock and primary shock reflection. As the the reflected planar shocks travel further downstream, the transverse compression surface provides additional compression with a x-y planar shock in the z-direction, as denoted by the blue surface. This shock system will be referred to as the secondary shock and secondary shock reflection. The actual shock system in the three-dimension model is similar to that of the simplified model, and can be seen in Figure 2b. The primary and secondary shock systems, again noted by the green and blue surfaces, are observed to be nearly planar even though the compression surfaces are highly three-dimensional.

To this point in the design process the flow-field has been assumed to be inviscid and laminar, which is a poor assumption based on the freestream conditions. Due to the magnitude of the freestream Reynolds number, it is expected that transition will occur well upstream of the primary compression shock and the boundary layer is assumed to be fully-turbulent. To attempt to correct for the growth of the turbulent boundary layer, analytic corrections based on localized momentum thickness are applied along the calculated streamlines. As the boundary layer develops, it effectively increases the contraction ratio of the inlet, hence the analytic correction attempts to compensate by increasing the physical cross-sectional area.

The paired invisicid stream-trace/viscous correction method is extremely simple to implement, and can rapidly produce multiple geometries optimized for various flight conditions. However, a major trade-off for the simplicity of a streamline-traced method is the inability to predict viscous nonlinear interactions, primarily shock-boundary layer interactions. The multiple-axis compression system produces a shock-dominated flow in the downstream end of the inlet, and the result of the primary and secondary shock on the incoming boundary layer and vice versa could prove to have a significant effect on the performance of the inlet. For this reason a higher fidelity numerical simulation needs to be performed on the inlet design before an experimental test is considered.

Computational Analysis

Computational analysis of the JAWS inlet design was performed for three reasons: to verify the design methodology of 1) stream tracing and 2) application of viscous corrections, and 3) to identify non-linear

Table 1: **JAWS4 Grid Parameters**

Grid	ξ_{max}	η_{max}	ζ_{max}	npts	δ_{min}
Inviscid	177	24	99	4.2E5	1e-3
Viscous (coarse)	235	76	101	1.8E6	1e-5
Viscous (fine)	391	126	201	9.9E6	1e-5

viscous effects not captured by the analytical design method which could have a negative impact on the performance of the inlet.

The first step towards design verification was to create three-dimensional models of the inlet geometry based on the coordinates described by the inviscid stream-trace and viscous-corrected stream-trace. Three computational meshes as described in Table 1 were then generated on the interior of the geometry. While quarter or half section grids using symmetry conditions could have been used to save computational resources, it was decided that fully three-dimensional grids would be used to allow for future yaw and pitch investigations.

For all simulations the research code FDL3DI was used to solve the full three-dimensional unsteady, Reynolds-Averaged Navier-Stokes (RANS) equations in strong conservation form using generalized coordinates. Closure to the system of equations is accomplished with the assumption of a perfect gas, a constant Prandtl number, and Sutherland's formula for molecular viscosity. Inviscid fluxes were solved to third-order accuracy using the Roe finite difference scheme and a $\kappa = 1/3$ MUSCL extrapolation. Viscous fluxes were solved using a standard second-order central difference method. An implicit Beam-Warming time integration scheme is used for temporal integration, while the effects of turbulence are handled by a two-equation k-ϵ turbulence model with low Reynolds number terms and a compressibility correction[7]. Further details of FDL3DI can be found in reference [8].

FDL3DI is a structured-grid solver, which allows for greater fidelity and numerical efficiency than a comparable unstructured solver, but adds complexity to grid generation. A generalized coordinate framework requires the physical grid geometry to be mappable to a rectangular topology, which is relatively straightforward for simple external surfaces. For internal flow through a circular cross section, topology definition requires one of two options: the "rounding" of the corners of a rectangular domain to fit within the inlet, or the "wrapping" of a domain around the interior of the inlet similar to an o-type grid. The first option allows for a uniform mesh at the interior of the domain, but creates highly skewed cells with poor aspect ratios at the outermost surfaces. The second option allows for a uniform outer surface and simplified η_{max} boundary condition, but creates a singularity where all η-minimum coordinates collapse to a single line. For this work the second option was chosen to ensure the outer surfaces were as uniform as possible to most closely match the desired inlet geometry. No large-scale influence of the centerline singularity on the solution was seen, but additional studies are investigating the use of an overset rectangular section to eliminate the possibility of localized errors due to spatial averaging.

The first series of calculations ignoring viscous and turbulent contributions to the governing equations were performed on the inviscid geometry to verify the location of the primary and secondary shock surfaces. A second series of calculations were then performed on the viscous-corrected geometry with the turbulence modeling enabled. The differences in the structure of the inviscid and turbulent flow-fields can be seen in slices along the X-Y centerline planes in Figure 3. The upstream primary shock and primary reflection are well defined, with the primary reflection reaching the external surface of the inlet very near to the desired location for both the inviscid and turbulent cases. The vertical contour line seen downstream in both cases is the reflection of the secondary compression shock 90 degrees out of plane. However, in the inviscid (top) case the shock reflection is uniform along the height of the inlet, while a new structure can be seen developing at the intersection for the turbulent (bottom) case. The growth of these two opposing lower-momentum regions can be seen looking at an X-Z plane at the combustor interface of Figure 4. It is worth noting that the average Mach number based on total velocity magnitude across the exit plane is very similar for both

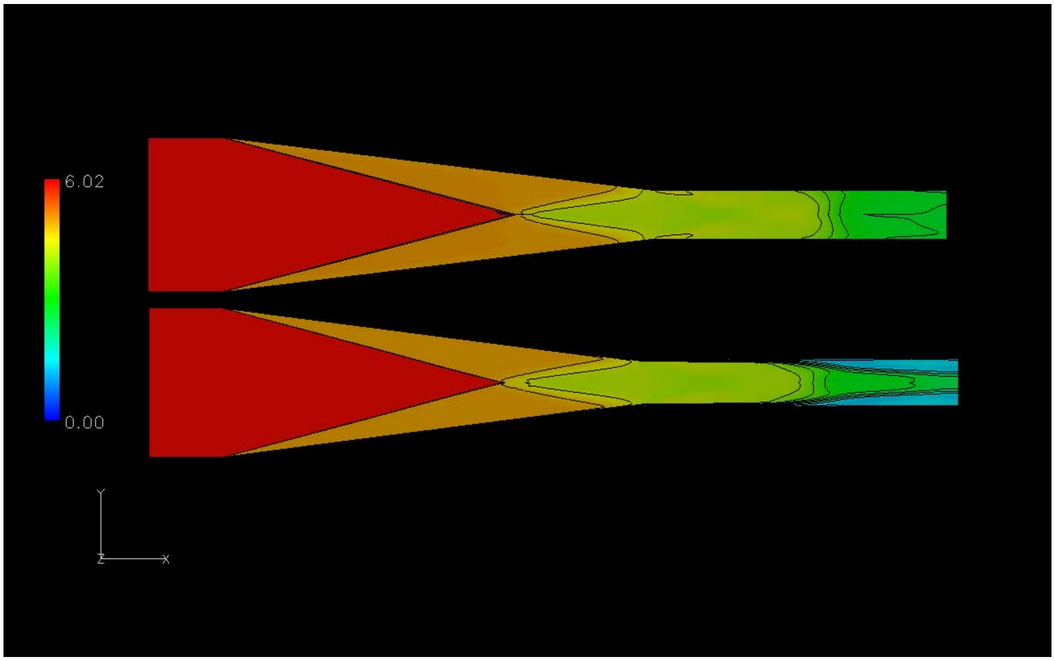

Figure 3: **Mach number contours, inviscid (top) and turbulent (bottom), along X-Y center plane.**

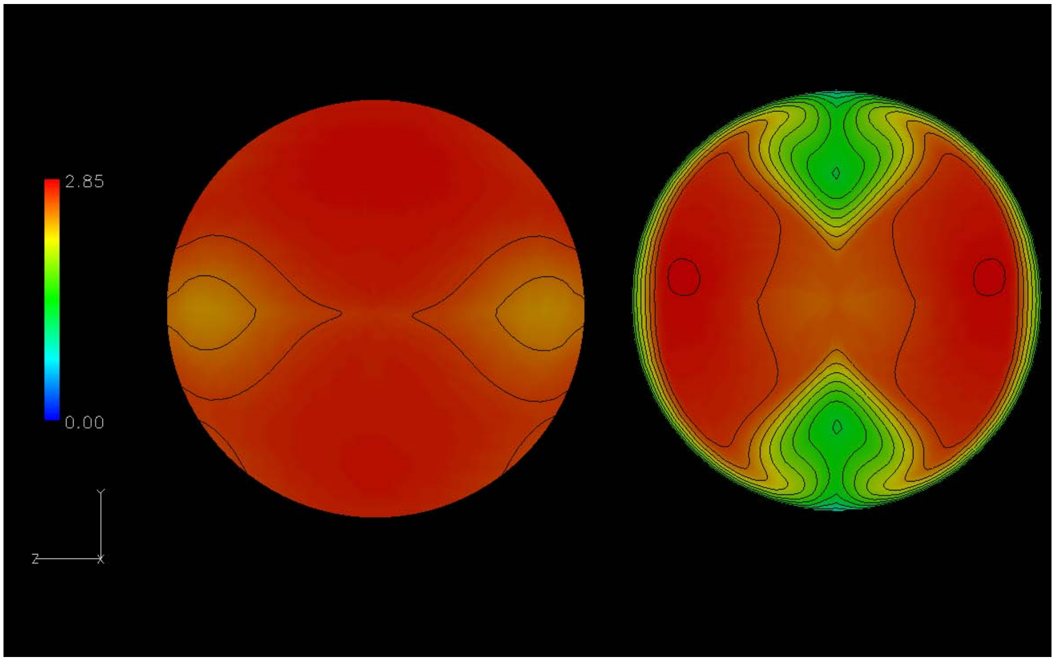

Figure 4: **Mach number contours at exit plane, inviscid (left) and turbulent (right).**

cases, meaning there is a significant amount of non-streamwise velocity introduced into the flow by these new structures.

Further investigation has identified that the cause of these structures is the swept-shock boundary-layer interaction of the secondary compression shock and the developed boundary layer on the top and bottom of the inlet. This canonical interaction has been studied in depth experimentally by Zheltovodov[9] and computationally by Gaitonde et al.[10, 11, 12] on the double-fin, and is frequently seen in sidewall compression inlets. The primary effect of the swept-shock interaction is the localized separation of the boundary layer and the formation of multiple vortical structures which propagate downstream into the combustor interface. Figure 5 shows the centerline Mach number along the length of the inlet. The influence of the primary and secondary shocks are clearly seen in both results, yet the impact of the swept shock interaction for the viscous case is minimized along this axis. Should the magnitude of this interaction be strong enough, it is possible that the detached boundary layer would cause significant flow blockage resulting in an inlet unstart. However, for this particular geometry the separated boundary layer does not penetrate completely into the core flow but is localized into two distinct detached vortex structures.

The lower half-section cutaway in Figure 6 highlights five distinct components of the interaction: a separated boundary layer (purple and red), centerline vortex (turquoise), vortex interactions (yellow), and entrainment flow (blue). As flow enters the secondary compression shock region, the incoming boundary layer flow separates and does not reattach. A line of primary coalescence sweeps from near the fin leading edge to the centerline plane of symmetry. As the boundary layer separates, it narrows and allows for the creation of the other flow elements. Fluid which attaches near the compression corner is swept spanwise and then separates from the underside of the separated boundary layer, creating the vortex interaction region. Other fluid, originating near the compression leading edge, is also swept spanwise but then turned streamwise to form a pair of vortical structures. Finally, incoming flow in the invisicid region near the compression leading edge attaches near the corner then also sweeps spanwise towards the centerline region.

The primary effect of the swept-shock interaction is a localized increase in surface pressure and surface heating along the lines of separation and attachment. The maximum heating is expected to occur downstream in the vortex interaction region, where peak heating rates can be 10 to 20 times greater than quiescent regions[13]. This increase in pressure and heat transfer can be particularly damaging from a structural viewpoint, where it can significantly reduce material lifespan. However, when analyzing the swept-shock interaction in a numerical simulation it is important to note that the choice of turbulence model can strongly influence the predicted interaction strength. Studies of the double-fin configuration have demonstrated numerical simulations can accurately match experimental data in attached regions of the flow, but greatly over-predict surface pressure and heat transfer after separation due to limitations of turbulence modeling[14]. If the model is overly-diffusive and tends to delay boundary layer separation, the swept-shock interaction will be under-predicted and a blockage effect could be overlooked. Likewise, a model which over-predicts separation could cause premature blockage and unjustified unstart concerns. Thus, the exact behavior of the shock-boundary layer interaction can only be accurately predicted after comparison with carefully chosen experimental data.

Experimental Test Program

The final phase of the JAWS inlet design is the fabrication of a test article to be flown in the NASA Langley 20” Mach 6 aerothermodynamic wind tunnel. A test entry was originally scheduled for the spring of 2007, but due to competing priorities at NASA has been rescheduled. Hence, no experimental data was available at the time that this paper was written. It is anticipated that the test series will be completed in late 2007 and the comparison of experimental results will be presented at a later date.

The primary purpose of the experimental test series is to verify the analytical design tools and validate the performance of the computational predictions. These objectives will be accomplished by the careful selection of instrumentation on the experimental model. A major challenge in inlet testing is visualization of the internal flow-field. Since the performance of the inlet is tied directly to the internal flow-path geometry, the intrusion of diagnostic instrumentation could adversely affect the resulting internal flow structure. For

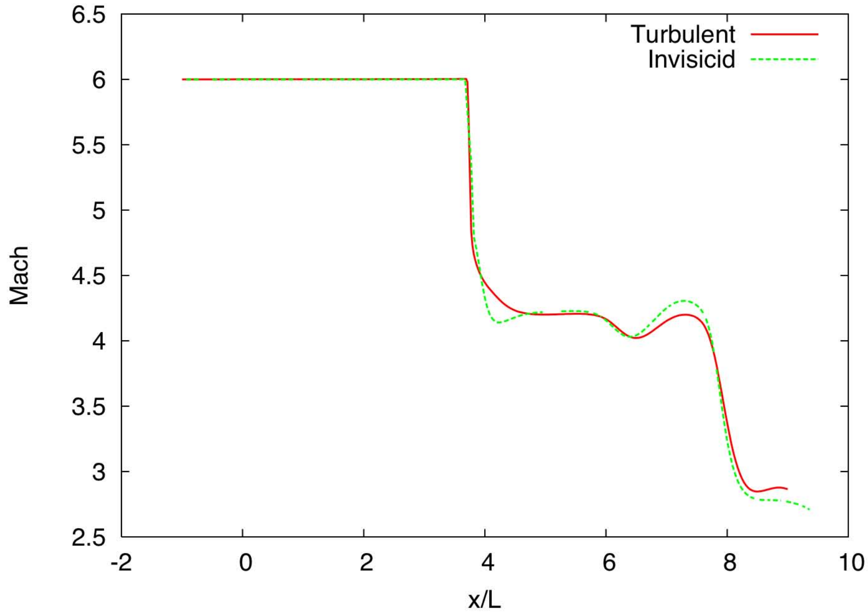

Figure 5: **Centerline Mach number for inviscid and turbulent solutions.**

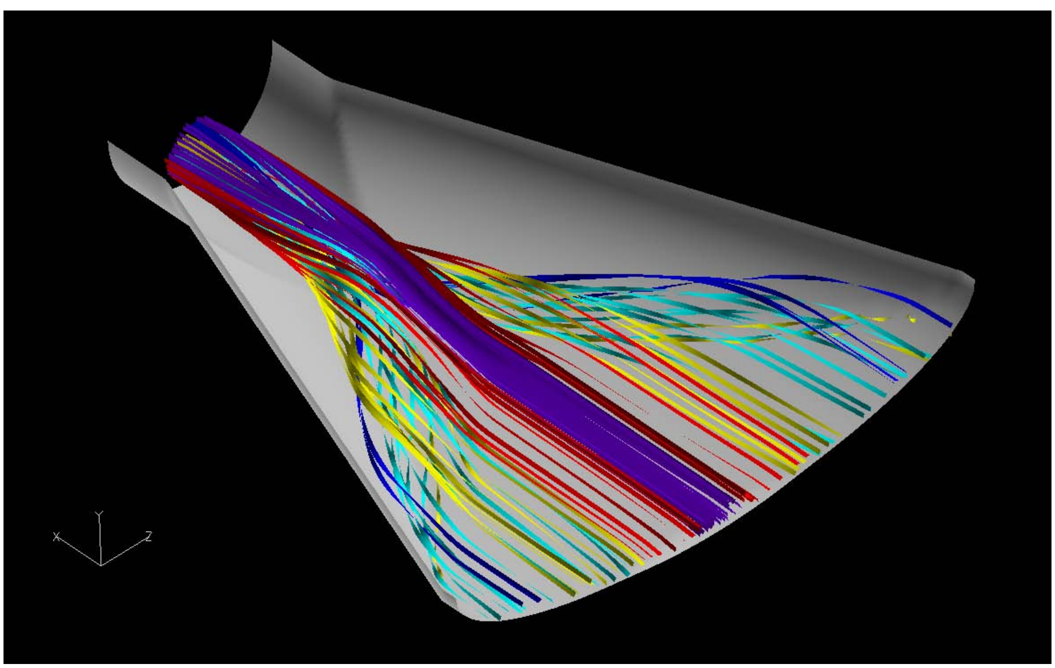

Figure 6: **Swept-Shock Boundary Layer Interaction in lower half of turbulent JAWS inlet.**

Table 2: **JAWS4 Test Objectives**

Test Series	Purpose	Method
1	Inlet Starting	Variations in Injection rate, α, β
2	Identify Operability Limits	α, β sweeps
3-6	Collect Performance Data	Finite α, β
7	Operability Extremes	P_t, T_t, Re, variations
8	Oil surface flow visualization	

this reason, no internal probes will be used but only static pressure and temperature measurements at various locations on the internal surface of the model.

The computational fluid dynamic simulations were completed on the viscous geometry prior to final model fibrication, and instrument measurement locations were determined based on areas of interest from the numerical results. A series of equal spaced pressure ports were placed along specific surface streamlines to attempt to capture the pressure gradients along the primary and secondary shock structures, as well as several sets of circumferential groups at various up and downstream locations to quantify the location of the pre-and-post swept shock interaction. It is expected that the data collected in the upstream regions of the inlet will match the predicted values well, as the flow is well behaved and primarily inviscid. The matching of computational and experimental data in the downstream regions where the swept-shock interaction is predicted should be of more of a challenge due to the complexity of the interaction and the uncertainty in the turbulence modeling. To provide further insight in these regions of complex phenomena, a surface oil-flow technique will also be applied to selected tests to attempt to qualitatively measure the separation and reattachment patterns inside of the inlet.

In addition to instrumentation on the interior of the inlet, the flow-field distortion across the exit plane will be measured with a custom cruciform pitot probe. While there is no official standard for hypersonic inlets, SAE ARP-1420 for traditional inlets should still be applicable[15]. Per the recommended standard, forty area-weighted pressure measurements will be taken across the exit plane face. Any computational inaccuracies introduced by the turbulence model should be manifest in the distortion field driven primarily by the detached vortices of the swept-shock interaction.

The experimental test series will also investigate both on and off design performance of the inlet, including variations of yaw, pitch, and mach number as listed in Table 2. Since the JAWS design utilizes fixed-geometry, it is critical to understand its performance at conditions other than ideal for maximum military utility.

Conclusions & Future Work

A circular cross-section inward-turning hypersonic inlet has been designed to produce specific performance characteristics. The inlet features a circular profile at the leading edge and combustor interface yet compression is accomplished primarily with planar shocks. Its design was generated using an invisicid streamline tracing method with an analytical correction for turbulent boundary layer growth. Computational fluid dynamics simulations were used to verify the analytic tools and predict the influence of nonlinear effects. Comparison of the viscous and inviscid results demonstrated shortfalls of the simplified assumptions through fundamental differences in the downstream flow-fields. The computational simulation predicated a separated boundary layer and vortex formation due to the swept shock interaction at the downstream shock location, but overall performance is still anticipated to be within acceptable limits. A wind tunnel test article was fabricated and instrumented using insight gained from the numerical studies. It is scheduled to be flown in a NASA hypersonic wind tunnel in late 2007, and should provide validation of the performance predicted by the numerical simulations.

Future comparison of the computational and experimental results will provide insight on the ability of numerical models to accurately predict hypersonic inlet design performance. With this information the limitations of the current simplified design process can be overcome through new analytical methods, allowing for better initial estimates of overall performance and increased confidence in hypersonic inlet design tools.

Acknowledgments

The author would like to thank P. Kutshenreuter and H. Meicenheimer for their JAWS modeling and design support, and D. Gaitonde for his technical leadership and many useful discussions. This project is sponsored in part by the Air Force Office of Scientific Research (monitored by J. Schmisseur), and by a grant of High Performance Computing time from the Department of Defense Major Shared Resource Centers at the Aeronautical Systems Center (ASC).

References

[1] Malo-Molina, F., Gaitonde, D., and Kutschenreuter, P., "Numerical Investigation of an Innovative Inward Turning Inlet," AIAA paper 2005–4871, 2005.

[2] Smart, M. K., "Experimental Testing of a Hypersonic Inlet with Rectangular-to-Elliptical Shape Transition," *AIAA Journal of Power and Propulsion*, Vol. 17, No. 2, 2001, pp. 276–283.

[3] Smart, M. K. and Trexler, C. A., "Mach 4 Performance of Hypersonic Inlet with Rectangular-to-Elliptical Shape Transition," *AIAA Journal of Power and Propulsion*, Vol. 20, No. 2, 2001, pp. 288–293.

[4] Smart, M. K., "Design of Three-Dimensional Hypersonic Inlets with Rectangular-to-Elliptical Shape Transistion," *AIAA Journal of Power and Propulsion*, Vol. 15, No. 3, 1999, pp. 408–417.

[5] Lindsey, M. F., McMullan, R. J., and Gaitonde, D. V., "Development of a Realistic 3-D Scramjet Flowpath for MGD Energy Bypass," AIAA paper 2005–1178, 2005.

[6] Kutshenreuter, P., "Testing of Hypersonic Inlets in Helium and Air," Tech. rep., General Electric Company Advanced Engine and Technology Department, Cincinnati, Ohio, June 14-18 1965, Presented at the AIAA Propulsion Joint Specialist Conference, United States Air Force Academy, Colorado.

[7] Rizzetta, D. P., "Numerical Simulation of Turbulent Cylinder Juncture Flowfields," AIAA paper 93-3038, 1993.

[8] Gaitonde, D. V. and Visbal, M. R., "High-Order Schemes for Navier-Stokes Equations: Algorithm and Implementation into FDL3DI," AFRL-VA-WP-TR-1998-3060, 1998.

[9] Zheltovodov, A. A. and Maksimov, A. I., "Hypersonic Crossing-Shock-Wave/Turbulent Boundary Layer Interactions Technical Report Final Report," Eoard contract F61775-98-WE091, Russian Academy of Sciences, Novosibirsk, Russia, 1999.

[10] Gaitonde, D. V., Shang, J. S., Garrison, T. J., Zheltovodov, A. A., and Maksimov, A. I., "Evolution of the Seperated Flow Field in a 3D Shock-Wave/Turbulent Boundary-Layer Interaction," AIAA paper 1997-1837, 1997.

[11] Gaitonde, D. and J.S.Shang, "On 3D Shock-Wave/Turbulent Boundary-Layer Interactions at Mach 4," AIAA paper 1996-0043, 1996.

[12] Gaitonde, D. and Shang, J. S., "Structure of a Turbulent Double-Fin Interaction at Mach 4," *AIAA Journal*, Vol. 33, No. 12, 1995, pp. 2250–2258.

[13] Croker, B. A., "Numerical Investigation of 3-D Swept Shock Interaction Control with Porous Surfaces," AIAA paper 2006–3346, 2006.

[14] Schmisseur, J. and Gaitonde, D., “Numerical Investigation of New Topologies in Strong Crossing Shock-Wave/Turbulent Boundary-Layer Interactions,” AIAA paper 2000-0931, 2000.

[15] “ARP-1420 Gas turbine engine inlet flow distortion guidelines,” SAE Committee S-16.